



<b>Title</b>	<b>A study of In<sub>x</sub> Ga<sub>1-x</sub> N growth by reflection high-energy electron diffraction</b>
<b>Author(s)</b>	<b>Liu, Y; Xie, MH; Cao, YG; Wu, HS; Tong, SY</b>
<b>Citation</b>	<b>Journal Of Applied Physics, 2005, v. 97 n. 2</b>
<b>Issued Date</b>	<b>2005</b>
<b>URL</b>	<b><a href="http://hdl.handle.net/10722/42501">http://hdl.handle.net/10722/42501</a></b>
<b>Rights</b>	<b>Creative Commons: Attribution 3.0 Hong Kong License</b>

# A study of $\text{In}_x\text{Ga}_{1-x}\text{N}$ growth by reflection high-energy electron diffraction

Y. Liu, M. H. Xie,<sup>a)</sup> Y. G. Cao, and H. S. Wu

*Department of Physics and HKU-CAS Joint Laboratory on New Materials, The University of Hong Kong, Pokfulam Road, Hong Kong, China*

S. Y. Tong

*Department of Applied Physics and Materials Science, City University of Hong Kong, Tat Chee Avenue, Kowloon, Hong Kong, China*

(Received 6 July 2004; accepted 2 November 2004; published online 22 December 2004)

Epitaxial growth of  $\text{In}_x\text{Ga}_{1-x}\text{N}$  alloys on GaN(0001) by plasma-assisted molecular-beam epitaxy is investigated using the *in situ* reflection high-energy electron-diffraction (RHEED) technique. Based on RHEED pattern changes over time, the transition of growth mode from two-dimensional (2D) nucleation to three-dimensional islanding is studied for various indium compositions. RHEED specular-beam intensity oscillations are recorded during the 2D wetting-layer growth, and the dependences of the oscillation period/frequency on the substrate temperature and source flux are established. By measuring the spacing between diffraction spots in RHEED, we also estimated indium composition,  $x$ , in alloys grown under different flux combinations. Incorporation coefficients of both gallium and indium are derived. Possible surface segregation of indium atoms is finally examined. © 2005 American Institute of Physics. [DOI: 10.1063/1.1840101]

## I. INTRODUCTION

III-V nitrides continue to attract people's attention due to their promises in optoelectronic applications.<sup>1,2</sup> Recent studies have indicated that the energy-band gap of InN is much smaller than previously thought.<sup>3-5</sup> Therefore, by tuning the indium (In) composition in an InGaN alloy, the whole visible spectral range can arguably be covered by the nitride system. However, due to a large difference in atomic size between In and gallium (Ga) atoms, and due to the differences in thermal-expansion coefficients and mechanical properties between InN and GaN, the growth of  $\text{In}_x\text{Ga}_{1-x}\text{N}$  with precise compositional control has been shown to be difficult. There can be phase separation and composition fluctuation in the epilayer.<sup>6,7</sup> Also, the constituent species may interfere with each other in their incorporation kinetics.<sup>8-10</sup> Therefore, it remains challenging to fabricate high-quality  $\text{In}_x\text{Ga}_{1-x}\text{N}$  layers in the whole composition range ( $0 \leq x \leq 1$ ).

In this paper, an investigation of  $\text{In}_x\text{Ga}_{1-x}\text{N}$  growth by plasma-assisted molecular-beam epitaxy (PA-MBE) is carried out using the *in situ* reflection high-energy electron-diffraction (RHEED) technique. The evolution of both the RHEED pattern and the specular-beam intensity is monitored in order to determine the growth mode and deposition rates. By measuring the distance between neighboring diffraction spots in RHEED, the lattice parameter and thus the indium composition in the alloy are estimated for different flux combinations. The incorporation coefficients for Ga and In are derived. Some possible surface segregation of In atoms during growth is also examined.

## II. EXPERIMENTS

The experiments were conducted in a multichamber ultrahigh-vacuum (UHV) system, in which the PA-MBE re-

actor was connected under vacuum with some surface characterization facilities, such as a scanning tunneling microscope (STM), via UHV interlocks.<sup>11</sup> Conventional effusion cells for Ga and In and a radio-frequency nitrogen (N) plasma unit were installed in the MBE chamber. The chamber was also equipped with a RHEED gun operating at 10 kV. For nitride epitaxial growth, *n*-type 6H-SiC(0001) wafers were used as substrates. They were first treated by thermal heating under a silicon flux in order for the  $(\sqrt{3} \times \sqrt{3})R30^\circ$  surface reconstruction to appear. Then GaN was deposited at 600 °C under the excess-Ga condition.<sup>11</sup> After growing a thick film (0.5–1.0  $\mu\text{m}$ ), the surface was briefly annealed at 600 °C to remove surface Ga atoms in excess. Then,  $\text{In}_x\text{Ga}_{1-x}\text{N}$  deposition was initiated at lower substrate temperatures (350–580 °C) using different source fluxes. Sample heating was achieved by applying a direct current through the long side of the rectangular sample piece. The error in sample temperature reading as measured by a focal infrared pyrometer was less than 10 °C. The effusion cell temperatures were measured by thermocouples in contact with *p*BN crucibles, and the fluxes of Ga, In, and active N were calibrated through the measurements of the growth rates of GaN and InN in the metal-rich and N-rich regimes, respectively.<sup>11</sup> During alloy deposition, RHEED patterns and their specular-beam intensities were recorded by a charge-coupled device (CCD) camera and analyzed by the KSA-400 software in a personal computer. For selected samples, surface morphologies were examined by STM at a tunneling current of 0.1 nA and a sample bias of –2.5 V. Secondary-ion-mass spectrometry (SIMS) measurements were also carried out for In concentration profile using a Physical Electronics PHI 7200 ToF-SIMS spectrometer. The primary beam was 8-keV cesium ( $\text{Cs}^+$ ), which was focused on the sample at an angle of 60° off the surface normal.

<sup>a)</sup>Author to whom correspondence should be addressed; electronic mail: mhxie@hkusua.hku.hk

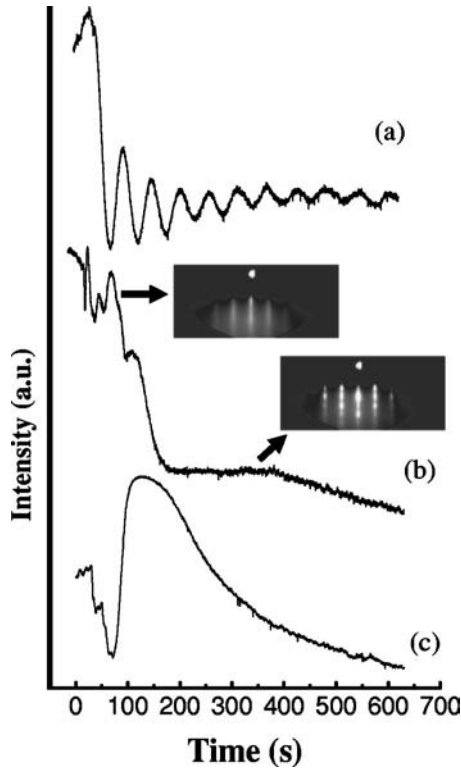


FIG. 1. RHEED specular-beam intensity oscillations during deposition of  $\text{In}_x\text{Ga}_{1-x}\text{N}$  on  $\text{GaN}(0001)$  at  $460^\circ\text{C}$  under the following fluxes: Ga:  $1.8 \times 10^{13}$  atoms/ $\text{cm}^2 \text{s}^{-1}$  (equivalent to a GaN deposition rate of 0.016 bilayers/s); N:  $7.0 \times 10^{13}$  atoms/ $\text{cm}^2 \text{s}^{-1}$  (equivalent to a growth rate of 0.062 bilayers/s for GaN); and In: (a)  $1.3 \times 10^{12}$ , (b)  $3.5 \times 10^{13}$ , and (c)  $7.6 \times 10^{13}$  atoms/ $\text{cm}^2 \text{s}^{-1}$  (corresponding to  $\text{InN}$  growth rates of 0.0015, 0.045, and 0.054 bilayers/s, respectively). The insets show representative RHEED patterns at different growth stages.

### III. RESULTS AND DISCUSSIONS

#### A. RHEED oscillations and film growth rates

RHEED specular-beam intensity oscillations are recorded during the growth of  $\text{In}_x\text{Ga}_{1-x}\text{N}$  on  $\text{GaN}(0001)$ . Figure 1 shows a few examples for different source fluxes. Except for low In fluxes, where sustained oscillations are observed with gradually diminishing amplitudes, a limited number of oscillation periods are obtainable for high In to Ga flux ratios. A transition of the RHEED pattern from

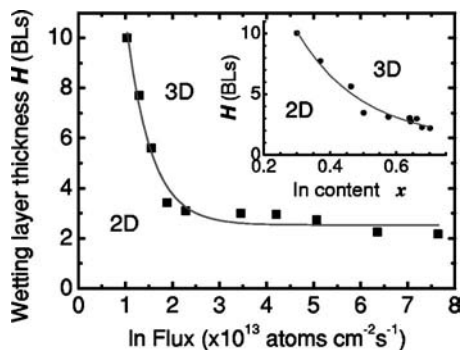


FIG. 2. 2D wetting-layer thickness  $H$  as a function of the In source flux  $F_{\text{In}}$  or In composition  $x$  in alloy (inset). The values of  $x$  are estimated based on the strain in the film (refer to Fig. 8). The growth temperature was  $460^\circ\text{C}$ . The Ga and N fluxes are  $1.8 \times 10^{13}$  and  $7.0 \times 10^{13}$  atoms/ $\text{cm}^2 \text{s}^{-1}$ , respectively. The line is drawn to guide the reader's eyes.

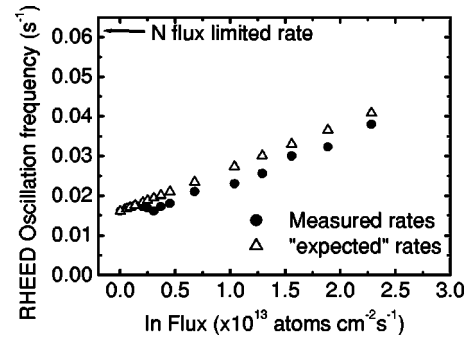


FIG. 3. RHEED oscillation frequency measured during  $\text{InGaN}$  wetting-layer growth under different In fluxes (filled circles). The “expected” growth rates according to source fluxes are shown by empty triangles, assuming unit incorporation coefficients for Ga and In. The flux of Ga was constant at  $1.8 \times 10^{13}$  atoms/ $\text{cm}^2 \text{s}^{-1}$ , while the N flux was  $7.0 \times 10^{13}$  atoms/ $\text{cm}^2 \text{s}^{-1}$ . The growth temperature was  $460^\circ\text{C}$ .

streaks to spots is associated with it (see the insets), indicating a growth mode change from two-dimensional (2D) nucleation to three-dimensional (3D) islanding, characteristic of the Stranski–Krastanow growth mode. Increasing the flux of In leads to fewer oscillations and thus to a thinner wetting layer of  $\text{In}_x\text{Ga}_{1-x}\text{N}$  on GaN. Assigning each oscillation period to one bilayer (1 bilayer =  $c/2$ , where  $c$  is the lattice constant in the  $[0001]$  direction), we summarize in Fig. 2 the dependence of the wetting-layer thickness on the In flux for fixed Ga and N fluxes and a constant substrate temperature of  $460^\circ\text{C}$ . As will be shown later, changing the In flux leads to different In compositions in the alloys. Therefore, Fig. 2 also corresponds to a dependence of the wetting-layer thickness on the In composition  $x$ , as shown in the inset of the figure. Note that changing the growth temperature may lead to adjustments in the dependence, but the general trend remains the same, which is in agreement with the literature.<sup>12</sup>

Figure 3 plots the RHEED oscillation frequencies during the growth of the wetting layer as a function of the In flux at  $460^\circ\text{C}$ , while Fig. 4 shows data as a function of the substrate temperature. In Fig. 3, the “expected” growth rates corresponding to the source fluxes are also shown, assuming that the incorporation coefficients for both Ga and In are unity. From the figure, one immediately notes that the measured RHEED oscillation frequencies do not always correlate to the supplied fluxes. Rather, the measured oscillation frequencies are lower than the expected growth rates for high In

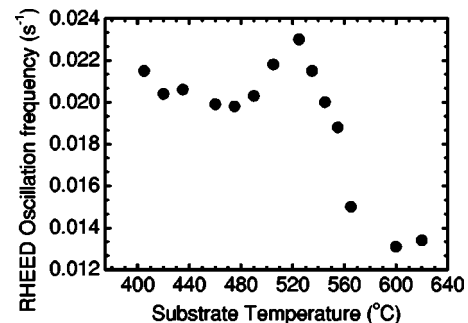


FIG. 4. RHEED oscillation frequency measured during  $\text{InGaN}$  wetting-layer growth at different substrate temperatures. The fluxes of Ga, In, and active N are  $1.8 \times 10^{13}$ ,  $6.8 \times 10^{13}$ , and  $7.0 \times 10^{13}$  atoms/ $\text{cm}^2 \text{s}^{-1}$ , respectively.

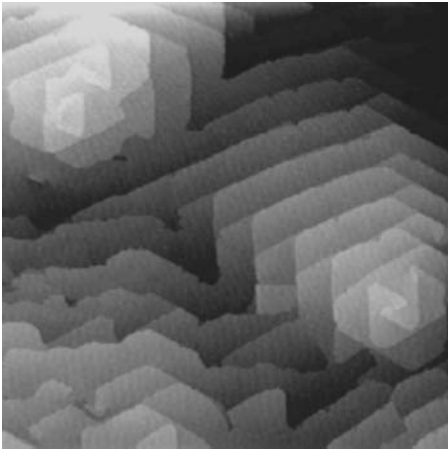


FIG. 5. STM image showing a surface of the starting GaN(0001), on which InGaN is deposited and the RHEED intensity oscillations recorded. Image size:  $1000 \times 1000 \text{ nm}^2$ .

fluxes. There can be two reasons for this observation. First, it may reflect diminished incorporation coefficients for In and/or Ga, therefore, the *growth rates* of the film become less than expected.<sup>8,9</sup> Second, the RHEED oscillation frequency *does not* correspond to the actual growth rate, which will be the case if growth proceeds by (partial) step flow on a vicinal surface.<sup>13–15</sup> Increasing the substrate temperature enhances the surface diffusion of adatoms and thus increases the probability of step-flow growth. Consequently, the RHEED oscillation frequency, which is characteristic of the 2D nucleation growth, progressively decreases as the deposition temperature increases.<sup>14,15</sup> For the InGaN growth carried out at a constant temperature, adding In on the surface may lead to similarly enhanced surface diffusion due to the surfactant effect of the In adlayer,<sup>8,16–18</sup> equivalent to increasing the substrate temperature. As a result, more atoms incorporate into the film via step flow rather than by 2D nucleation. The RHEED oscillation frequency therefore increasingly deviates from that associated with a pure 2D growth.<sup>14</sup>

It should, however, be pointed out that the step-flow-induced oscillation frequency drop occurs only for growth on vicinal surfaces. In this experiment, nominally flat substrate surfaces ( $\leq 0.5^\circ$  according to supplier's specification) have been used. So, the relevance of step flow to the diminished RHEED oscillations may appear questionable. Nevertheless, STM examinations of the samples reveal that the surfaces are populated by spiral mounds as shown in Fig. 5. The side-walls of the spiral mounds constitute steps and terraces.<sup>19,20</sup> They are therefore effectively vicinal surfaces locally in the length scale of thousands of angstroms. This length scale is beyond the coherent length of the RHEED, so the latter effectively samples a vicinal surface rather than globally a flat one.

As mentioned earlier, the other possibility for the reduced oscillation frequency is the suppressed incorporation of constituent species. This suggestion was previously put forward by Adelman *et al.* to explain a similar observation.<sup>8,9</sup> Particularly, it was postulated that surface In atoms suppressed Ga incorporation, so the overall growth

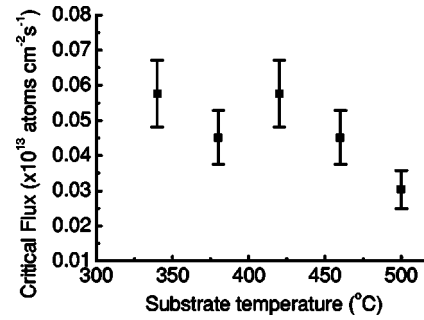


FIG. 6. Critical In flux, at which the RHEED oscillation frequency shows maximum drops from the “expected” growth rates, for various substrate temperatures.

rate of InGaN became less than the one of binary GaN for some critical In fluxes.<sup>8,9</sup> Considering the relatively stronger bonds between Ga and N than that between In and N, this would be a surprising result.

Irrespective of the causes, there seem to exist a critical In flux, beyond which the RHEED oscillation frequency starts to deviate from the expected growth rate of the film. We believe this may reflect the presence of a critical surface coverage of In atoms. Beyond this critical coverage, the surfactant effect of the In atoms becomes so significant that they have either caused an appreciable amount of step-flow growth or decreased incorporations of Ga and/or In. If this postulate is correct, increasing the substrate temperature will demand higher fluxes  $F$  in order to maintain the same critical coverage  $\theta = F\tau$ , as the adatom lifetime  $\tau$  decreases with the temperature. This speculation seems to agree with the experiments of Adelman *et al.*<sup>8,9</sup> However, our investigation did not produce a clear trend, as revealed in Fig. 6. If we accept that the observed drop in the RHEED oscillation frequency is due to the step-flow growth mode, increasing the temperature enhances step flow due to high thermal energy on the one hand, but reduces In coverage and so the surfactant-enhanced adatom diffusion on the other. Thus, the dependence of the critical flux on deposition temperature would be a complicated one.

Finally, the temperature dependence of the RHEED oscillation frequencies, as presented in Fig. 4, provides further insight to the problem. Below  $525^\circ\text{C}$ , changing the temperature affects the extent of step flow as well as the In surfactant coverage as argued above, therefore, it induces a nonmonotonic variation of the RHEED oscillation frequency. At temperatures above  $525^\circ\text{C}$ , step-flow growth becomes dominant and the incorporation of In and/or Ga is also reduced due to some dissociation of InN at high temperatures.

## B. In composition in alloy and the incorporation coefficients of Ga and In

We have followed the variations of distance  $D$  between (01) and (0 $\bar{1}$ ) diffraction spots in the RHEED pattern (see the inset of Fig. 7) as the growth of InGaN proceeds. It is shown to decrease from an initial value corresponding to the reciprocal of the lattice constant of GaN to a value corresponding to the reciprocal of the  $\text{In}_x\text{Ga}_{1-x}\text{N}$  lattice parameter with an In content  $x$ .<sup>21</sup> Using the measured values of  $D$  for thick

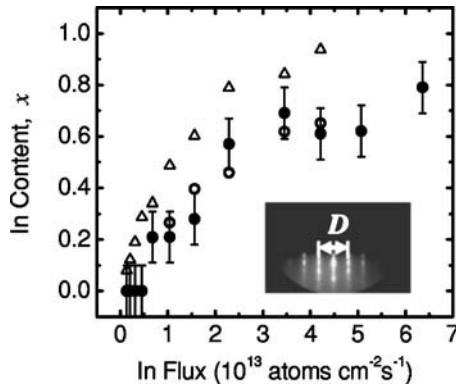


FIG. 7. Filled circles represent In content data deduced from distances  $D$  between  $(01)$  and  $(0\bar{1})$  diffraction spots in RHEED (see inset) for thick InGaN films, where strain relaxation is complete. Values calculated from the RHEED oscillation frequencies,  $f$ , are also given for comparison purposes. The data represented by “ $\circ$ ” are obtained according to  $x = (f_{\text{InGaN}} - f_{\text{GaN}}) / f_{\text{InGaN}}$ , whereas those represented by “ $\Delta$ ” are calculated according to  $x = f_{\text{InN}} / f_{\text{InGaN}}$ .

films where strain has been relieved, the alloy compositions,  $x$ , are estimated according to  $x = (a_{\text{InGaN}} - a_{\text{GaN}}) / (a_{\text{InN}} - a_{\text{GaN}}) = (D_{\text{GaN}} / D - 1) / (D_{\text{GaN}} / D_{\text{InN}} - 1)$  for various flux combinations, where  $a_{\text{InGaN}}$ ,  $a_{\text{GaN}}$ , and  $a_{\text{InN}}$  are the lattice constants for  $\text{In}_x\text{Ga}_{1-x}\text{N}$  alloy and binary GaN and InN, respectively.  $D$ ,  $D_{\text{GaN}}$ , and  $D_{\text{InN}}$  are the measured distances between  $(01)$  and  $(0\bar{1})$  diffraction spots for the alloy, for GaN, and for InN films. Obviously, the above formula assumes the validity of Vegard’s law. Figure 7 shows the results for varying In fluxes but fixed Ga and N fluxes at  $1.8 \times 10^{13}$  and  $7.0 \times 10^{13}$  at.  $\text{cm}^{-2} \text{s}^{-1}$ , respectively. The deposition temperature was  $460^\circ\text{C}$ . For comparison, values calculated from the RHEED oscillation frequencies,  $f$ , according to (i)  $x = (f_{\text{InGaN}} - f_{\text{GaN}}) / f_{\text{InGaN}}$  and (ii)  $x = f_{\text{InN}} / f_{\text{InGaN}}$  are also given. Note that since the oscillation rates of GaN and InN were obtained independently during homoepitaxy, some adjustments due to the atomic areal density change when growing alloys should be implemented. However, the data presented in Fig. 7 did not take into account this factor. Formula (i) obviously applies when Ga incorporation is preminent, whereas formula (ii) would be applicable if In incorporation predominates. If the two elements incorporate fully with equal rates, the two formulas will lead to the same result. By inspecting Fig. 7, one notes that formula (i) has produced results that are closer to the ones based on lattice-constant estimation, suggesting the predominance of Ga incorporation. This is understood by the stronger bond of Ga–N than that of In–N.

In Figs. 8(a) and 8(b), we have plotted the dependences of the In and Ga incorporation rates as a function of the supplying fluxes of the sources. The incorporation rates for In,  $\alpha_{\text{In}}$ , and for Ga,  $\alpha_{\text{Ga}}$ , are estimated from the alloy composition  $x$ , taking into account the compositional dependences of the atomic areal density on surface  $\rho$  (atoms/ $\text{cm}^{-2}$ ) and film growth rates  $R$  (bilayers/s), according to  $\alpha_{\text{In}} = Rx\rho$  and  $\alpha_{\text{Ga}} = R(1-x)\rho$ , respectively. All the data refer to growth under N-rich regime. Least-square fittings to the data by linear relations give rise to the incorporation coefficients, which are  $0.82 \pm 0.03$  and  $1.01 \pm 0.02$  for In and

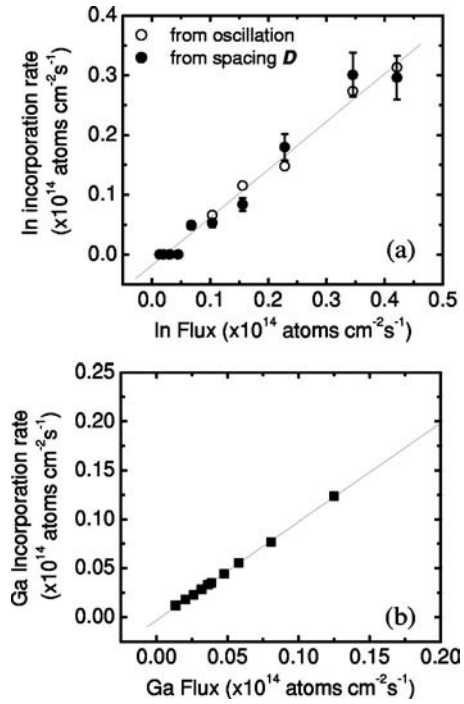


FIG. 8. Indium (a) and gallium (b) incorporation rates, calculated from the composition of the alloy, taking into account the dependence of surface areal density of atoms and film growth rates on composition  $x$ . The lines represent least-square fittings to the data. Note that in (a), two sets of data are given. One is derived from the  $x$  values measured from the spacing  $D$  in RHEED, whereas the other is from the values calculated from the RHEED oscillation frequencies,  $f$ , according to  $x = (f_{\text{InGaN}} - f_{\text{GaN}}) / f_{\text{InGaN}}$ . In (b), the data are derived solely from the oscillation frequencies using the above formula.

Ga, respectively. So, as suggested above by inspecting Fig. 7, incorporation of Ga is more efficient than that of In at the temperature investigated ( $460^\circ\text{C}$ ). In fact, the less-than-one incorporation coefficient for In is consistent with the presence of an In surfactant layer on the surface,<sup>16</sup> whose formation consumes some of the deposited In atoms from the flux. So, only a proportion of them incorporates into the film.

### C. In surface segregation

Finally, since In atoms have a large size, forming a surfactant wetting layer during alloy deposition, it is of interest to examine whether they segregate towards the surface during MBE.<sup>22,23</sup> To this end, we have grown a sample with three InGaN/GaN bilayers, the structure of which is illustrated in the inset of Fig. 9. The InGaN layers were grown under identical conditions (Ga, In, and N fluxes:  $1.8 \times 10^{13}$ ,  $3.7 \times 10^{12}$ , and  $2.5 \times 10^{13}$  atoms/ $\text{cm}^{-2} \text{s}^{-1}$ , respectively; substrate temperature:  $460^\circ\text{C}$ ), while the GaN capping layers were grown at progressively lower temperatures. The first one (i.e., the one closest to the substrate) was grown at  $550^\circ\text{C}$ . The second and the third GaN layers were deposited at  $500^\circ\text{C}$  and  $450^\circ\text{C}$ , respectively. The reason for choosing such a descending temperature sequence was to minimize the interdiffusion of atoms at InGaN/GaN interfaces. The In concentration profile in the sample was measured by means of the SIMS. The result is shown in Fig. 9. It is seen that the In concentration decreases in the GaN capping layers with similar rates (the decay lengths are measured to be 2.6, 3.1,

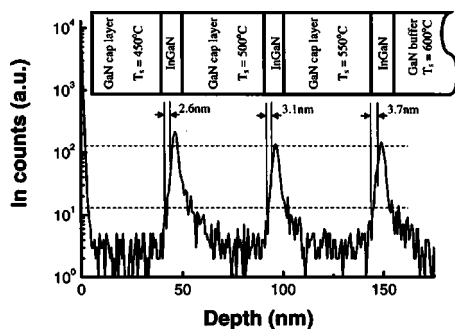


FIG. 9. In concentration profile measured by SIMS in a sample whose structure and growth condition are depicted in the inset. The nominal thickness of the InGaN alloy and GaN capping layers are 10 and 40 nm, respectively.

and 3.7 nm/decade, respectively, for the three front edges; see Fig. 9), very weakly dependent, if at all, on the GaN deposition temperature. Such a broadening might be due to progressively more important intermixing effect in SIMS. Hence, we may conclude that surface segregation of In is not that significant.<sup>22,23</sup> This result further reaffirms that the less-than-one incorporation coefficient of In is not due to some segregation effect.

#### IV. SUMMARY

RHEED intensity oscillations have been observed during InGaN deposition by PA-MBE. The apparent decrease in the oscillation frequency by adding some In is attributed to a gradual dominance of the step-flow growth mode. In and Ga incorporation coefficients have also been derived, which are shown to be unity for Ga but less than one for In under the N-rich growth regime. The less In incorporation coefficient is consistent with the formation of an In surfactant layer on surface. Therefore, only a proportion of the deposited atoms incorporate in the film while the rest contribute to the wetting-layer formation. Finally, possible surface segregation of In during growth is examined, which is shown to be low under the conditions investigated.

#### ACKNOWLEDGMENTS

We would like to acknowledge the technical support from W. K. Ho. The project is financially supported by grants from the Research Grants Council of the Hong Kong Special Administrative Region, China (Project Nos. HKU7118/02P and 7035/03P). One of the authors (M.H.X.) also acknowledges the support by National High-Tech Research and Development (863) Program of China under Grant No. 2003AA311060.

- <sup>1</sup>S. Strite and H. Morkoc, *J. Vac. Sci. Technol. B* **10**, 1237 (1992).
- <sup>2</sup>A. G. Bhuiyan, A. Hashimoto, and A. Yamamoto, *J. Appl. Phys.* **94**, 2779 (2003).
- <sup>3</sup>V. Y. Davydov *et al.*, *Phys. Status Solidi B* **229**, R1 (2002).
- <sup>4</sup>J. Wu *et al.*, *Appl. Phys. Lett.* **80**, 3967 (2002).
- <sup>5</sup>T. Matsuoka, H. Okamoto, M. Nakao, H. Harima, and E. Kurimoto, *Appl. Phys. Lett.* **81**, 1246 (2002).
- <sup>6</sup>R. Singh, D. Doppalapudi, T. D. Moustakas, and L. T. Romano, *Appl. Phys. Lett.* **70**, 1089 (1997).
- <sup>7</sup>M. K. Behbehani, E. L. Piner, S. X. Liu, N. A. El-Masry, and S. M. Behair, *Appl. Phys. Lett.* **75**, 2202 (1999).
- <sup>8</sup>C. Adelman, R. Langer, G. Feuillet, and B. Daudin, *Appl. Phys. Lett.* **75**, 3518 (1999).
- <sup>9</sup>C. Adelman, R. Langer, E. Martinez-Guerrero, H. Mariette, G. Feuillet, and B. Daudin, *J. Appl. Phys.* **86**, 4322 (1999).
- <sup>10</sup>T. Böttcher, S. S. Einfeldt, V. Kirchner, S. Figge, H. Heinke, D. Hommel, H. Selke, and P. L. Ryder, *Appl. Phys. Lett.* **73**, 3232 (1998).
- <sup>11</sup>S. M. Sean, M. H. Xie, W. K. Zhu, L. X. Zheng, H. S. Wu, and S. Y. Tong, *Surf. Sci.* **445**, L71 (2000).
- <sup>12</sup>N. Grandjean and J. Massies, *Appl. Phys. Lett.* **72**, 1078 (1998).
- <sup>13</sup>J. H. Neave, P. J. Dobson, B. A. Joyce, and J. Zhang, *Appl. Phys. Lett.* **47**, 100 (1985).
- <sup>14</sup>T. Shitara, J. Zhang, J. H. Neave, and B. A. Joyce, *J. Appl. Phys.* **71**, 4299 (1992).
- <sup>15</sup>J. Zhang (private communication).
- <sup>16</sup>J. Neugebauer, T. K. Zywiets, M. Scheffler, J. E. Northrup, H. Chen, and R. M. Feenstra, *Phys. Rev. Lett.* **90**, 056101 (2003).
- <sup>17</sup>C. Kruse, S. Einfeldt, T. Böttcher, and D. Hommel, *Appl. Phys. Lett.* **79**, 3425 (2001).
- <sup>18</sup>F. Widmann, B. Daudin, G. Feuillet, N. Pelekanos, and J. L. Rouvière, *Appl. Phys. Lett.* **73**, 2642 (1998).
- <sup>19</sup>M. H. Xie, L. X. Zheng, S. H. Cheung, Y. F. Ng, H. S. Wu, S. Y. Tong, and N. Ohtani, *Appl. Phys. Lett.* **77**, 1105 (2000).
- <sup>20</sup>M. H. Xie, S. M. Seutter, W. K. Zhu, L. X. Zheng, H. S. Wu, and S. Y. Tong, *Phys. Rev. Lett.* **82**, 2749 (1999).
- <sup>21</sup>Y. F. Ng, Y. G. Cao, M. H. Xie, X. L. Wang, and S. Y. Tong, *Appl. Phys. Lett.* **81**, 3960 (2002).
- <sup>22</sup>J. J. Harris, D. E. Ashenford, C. T. Foxon, P. J. Dobson, and B. A. Joyce, *Appl. Phys. A: Solids Surf.* **33**, 87 (1984).
- <sup>23</sup>M. H. Xie, J. Zhang, A. Lees, J. M. Fernandez, and B. A. Joyce, *Surf. Sci.* **367**, 231 (1996).

Journal of Applied Physics is copyrighted by the American Institute of Physics (AIP). Redistribution of journal material is subject to the AIP online journal license and/or AIP copyright. For more information, see <http://ojps.aip.org/japo/japcr/jsp>